

Greenhouse Window U-Factors Under Field Conditions

J. H. Klems, Ph.D.
Windows and Daylighting Group
Building Technologies Program
Environmental Energy Technologies Division
Ernest Orlando Lawrence Berkeley National Laboratory
University of California
Berkeley, California

June 1997

Greenhouse Window U-Factors Under Field Conditions

J. H. Klems, Ph.D.
Building Technologies Program
Environmental Energy Technologies Division
Ernest Orlando Lawrence Berkeley National Laboratory
Berkeley, CA

Abstract

Field measurements of U-factor are reported for two projecting "greenhouse" windows, each paired with a picture window of comparable insulation level during testing. A well-known calorimetric field test facility was used to make the measurements. The time-varying U-factors obtained are related to measurements of exterior conditions. For one of the greenhouse windows, which was the subject of a published laboratory hotbox test and simulation study, the results are compared with published test and simulation data and found to be in disagreement. Data on interior and exterior film coefficients are presented, and it is shown that the greenhouse window has a significantly lower interior film coefficient than a conventional window under the same interior conditions. This is advanced as a possible explanation of the disagreement.

Introduction

Windows are generally thought of as planar units, and their heat transfer is usually treated as one-dimensional (Arasteh, Reilly et al. 1993), or, more recently, two-dimensional (EE 1989; Finlayson et al. 1996). Certainly it is implicit in the design of hotbox tests of windows (Bowen and Solvason 1984; Bowen 1985; Elmahdy and Bowen 1988; Elmahdy 1992) and in their specification (NFRC 1991). Usually this picture is a reasonably good approximation of physical reality, but some products, such as skylights and projecting bay or "greenhouse" windows, are inherently three-dimensional and do not fit naturally into this scheme. Nevertheless, it is convenient for the building and components industry to treat the thermal specifications of these products also as if they were planar entities, so that design may handle all fenestration products in a uniform way. This formulates the problem of specifying the thermal performance of these products as (1) determining the net heat flow through the product under specified conditions, and (2) representing the product as a fictitious planar entity, expressing the heat flow in terms of this entity, and *defining conditions that make this planar entity analogous to an ordinary window*. The latter point is the source of some difficulty, as will be seen.

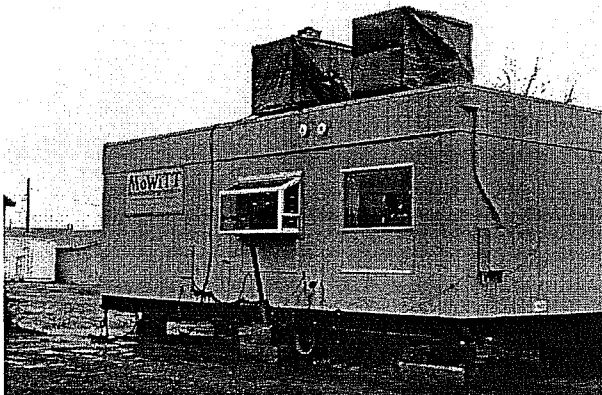


Figure 1. Greenhouse Window 1 and Comparison Double-Glazed Picture Window Mounted on Test Facility. The two windows are mounted on the side-by-side calorimeter chambers in a west-facing orientation; location is Reno, NV. The wall section below each window outlined in wood trim is the mask wall section used to adapt the windows to the chamber apertures. The two large blue-wrapped cubes on top of the facility are daylight simulation modules not used in this experiment. The wires below the greenhouse window are exterior sensors that had not yet been mounted on the windows when the photo was taken.

The geometry of a typical greenhouse window can be seen from the photo of Figure 1. Such a window projects out of the wall plane a distance significant in proportion to its height, consists of four vertical planar sections, a slanted top section, and a non-glazed bottom "shelf." Its total surface area may be in the range of two to four times the area of its rough opening. Theoretical calculation of the heat transfer through such an assembly for known surface conditions (i.e., a "C"-value calculation) presents no insuperable difficulties for the presently-existing array of tools: the various planar sections are treated separately by the usual one- or two-dimensional methods, in this way reducing the intrinsically three-dimensional segments (corners, etc.) to a small fraction of the total area for which relatively large uncertainties in heat transfer are tolerable. Two problems arise in choosing the surface ("boundary") conditions for the calculation, however. The normal practice is to assume constant film coefficients to represent the combined effects of convection and radiation, and to use these coefficients to link the surfaces to the interior and exterior air temperatures. But for a greenhouse window, the interior glass surfaces are radiatively linked together—one surface can "see" another (as well as the interior space, as in a normal "planar" window). Some of them are also convectively linked: under winter conditions, cold air from the vertical surfaces flows into the boundary layer for the lower "shelf," while the convection on the vertical surfaces will be affected by cold air from the tilted surface. For the exterior surface, the constant film coefficient is assumed to arise from the action of wind, but since a given wind speed and direction far from the window would be expected to produce different film coefficients for surfaces oriented in different directions relative to the wind direction, it is not clear what set of film coefficient assumptions for these surfaces correspond to the standard assumption made for a planar window.

Appeal to the usual measurement method, the hotbox test, does not resolve this problem, since the hotbox test procedures have been designed to model "typical extreme" conditions, and this modeling becomes uncertain for non-planar samples. Wind in a hotbox is most commonly applied in a direction normal to the window plane for a planar sample, in one type of test utilizing a calibration procedure to set the wind conditions (NFRC 1991) and in another type of test utilizing a "wind machine" designed to produce a known, constant exterior convective coefficient, on average (Elmahdy 1992). However, in the latter case an extremely non-planar sample does not allow the wind machine to operate in its intended fashion, and in both cases it is not possible so far to specify how the exterior conditions set up in the hotbox test of a greenhouse window relate to those for a planar sample, to the film coefficients to be used in a calculation, or to the conditions experienced under actual use of the window. Use of a wind flow parallel to the mounting plane, which is an alternative procedure more commonly used in Europe, does not improve matters.

In the face of this confusion it is necessary to return to field measurement in order to understand the relationship between U-factor, exterior conditions, and greenhouse window performance *vis-a-vis* planar samples. While requiring that more variables be measured (e.g., exterior radiant temperatures, as well as air temperatures and wind speed and direction), producing measurements under a variety of different conditions, and not allowing one to specify conditions at will, nevertheless field measurement represents the source of the present hotbox measurement conventions for planar samples and must be considered the final arbiter where those conventions need to be extended.

Methodology

Two greenhouse windows were measured in this project. Each greenhouse window sample was paired with a planar “picture” window fitting the same rough opening, and the two windows were measured side-by-side simultaneously. The picture window was chosen to have comparable insulation features (e.g., thermally unbroken or broken frame, type of glazing) to the corresponding greenhouse window.

Test Facility

Tests were conducted in an accurate, well-characterized, and well-known outdoor test facility (Klems, Selkowitz et al. 1982; Klems 1992) specifically designed for fenestration testing. This facility is shown in Figure 1 during the set-up period for the first of the tests. The test location was Reno, NV. Each of the calorimeter chambers is designed to measure the net heat flow through a fenestration as a function of time under realistic outdoor conditions. Consisting of dual, guarded, room-sized calorimeters in a mobile structure, the facility can simultaneously expose two windows to a room-like interior environment and to ambient outdoor weather conditions while accurately measuring the net heat flow through each window. This measurement comes from a net heat balance on each calorimeter chamber, performed at short intervals. To get an accurate net heat balance measurement and control the interior air temperature during the full diurnal cycle, each calorimeter chamber contains an electric heater, a liquid-to-air heat exchanger with measured flow rate and inlet/outlet temperatures, and a nearly continuous interior skin of large area heat flow sensors. There are also provisions for measuring all auxiliary electric power dissipated inside the chambers (e.g., fan power).

Sample Selection

The samples used in the tests are listed in Table 1. Greenhouse Window 1 is a sample used in an ongoing NFRC project, for which both hotbox test and simulation results have been published, (Carpenter and Elmahdy 1994) and for which further simulation work continues. Tests on this window were expected to provide the most reliable basis for comparing hotbox tests, field performance, and simulation. Since the significance of interior and exterior film coefficients becomes less as the intrinsic thermal resistance of the window increases, and since these film coefficients were expected to be the chief source of variability in performance, Greenhouse Window 2 with its comparison picture window was selected to provide performance information on a more thermally efficient unit.

Table 1. Test Samples

Test Period	Greenhouse Window	Picture Window
1	Double-glazed sealed-insulating glass panels, aluminum frame without thermal break; bottom uninsulated wood	Double-glazed with aluminum frame, no thermal break
2	Double-glazed low-E sealed insulating glass panels with Ar fill, vinyl frame	Double-glazed, low-E, Ar filled sealed insulating glass panel in vinyl frame

Sample Mounting

To mount the windows, which were nominally 1.5 m wide by 0.9 m high (5 ft X 3 ft), the mask wall normally used with the facility was removed from each of the two chambers, leaving a square aperture of approximately 1.5 m in each dimension. The samples were mounted in each chamber at the top of this aperture and a new mask wall consisting of 152 mm (6 in.) polystyrene foam faced with plywood was used to fill in the space (approximately 1.5 m X 0.6 m [5 ft X 2 ft]). The sample mounting is shown in Figure 2.

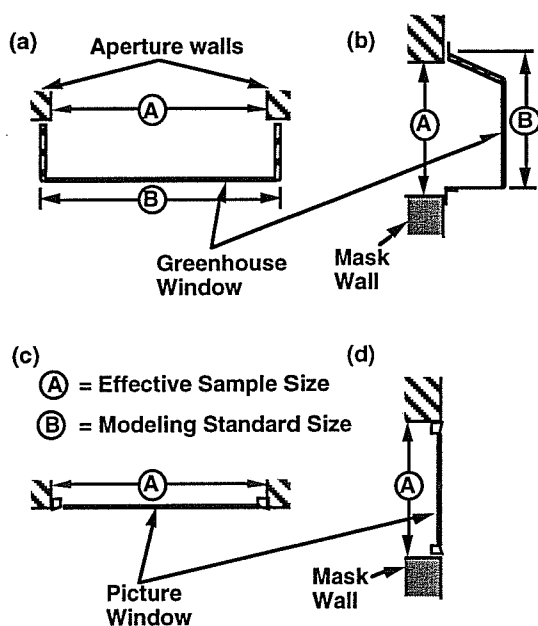


Figure 2. Sample Mounting. (a) Greenhouse window, horizontal section; (b) Greenhouse window, vertical section; (c) Picture window, horizontal section; (d) Picture window, vertical section.

Instrumentation

During the measurement associated instrumentation measures a variety of internal and external conditions: An array of thermistors with radiation shields monitors the average interior air temperature in each calorimeter, and an aspirated thermistor located in the on-site weather tower measures the exterior air temperature. A standard rotating-cup anemometer and weather vane measures the free-stream wind speed and direction. A sun-tracking pyrheliometer and a horizontally-mounted pyranometer measures beam and total horizontal solar intensity, respectively. Thermistors mounted on the glazing panels and frame members measure interior and exterior surface temperatures. A vertically-mounted pyranometer mounted above the two window samples measures the total solar (and ground-reflected) radiation intensity incident on the windows, and a vertically-mounted pyrgeometer measures the total incident long-wave infrared radiation (emitted by the sky and ground).

Data Analysis

All sensors in the facility were sampled rapidly by the controlling computer and their outputs stored. The sampling frequency varied with the type of sensor. These readings were then averaged and the results written to a data storage record each ten minutes. Approximately two hundred channels of information is normally accumulated in this way for each calorimeter chamber. Most of this information is used to monitor the facility operation.

The net heat flow through the sample was derived from the measurements for each ten-minute period by the method described in (Klems 1992). A two-dimensional finite-difference program (Childs 1991) was used to calculate the transient heat flow response factors for the mask wall, and these were combined with measured temperatures to determine the mask heat flow. (For the method, see Mitalas 1968.) For the data reported here this heat flow resulted in a small (<10%) constant correction to the measured U-factor of each sample. For each ten-minute period the U-value was calculated from the measured interior and exterior air temperatures, the net heat flow, and the effective sample area. For the picture windows the total area of the sample closely matched the test aperture opening area of 1.38 m². For the greenhouse windows, which mount on the outside of the wall, the “rough opening” size is somewhat a matter of definition (and application). Here a “Modeling standard rough opening” was chosen for each product to match the area used in simulating the products. (Arasteh, Finlayson et al. 1997)

Data were further combined into 30-minute averages, to suppress short-term weather fluctuations and to reduce the volume of information that needed to be studied.

Results

Figure 3 shows the U-factors obtained for each of the two test periods as a function of time. U-factors measurements were used only between the hours of 10 PM and 5:45 AM, in order to avoid the effects of solar gain. It is immediately apparent that the U-factor is not constant for any of the test specimens and varies both from night to night and within each night. For the second test period, nights 4-10 were selected for further examination, since they appeared to encompass the full range of U-factor variation shown in the test.

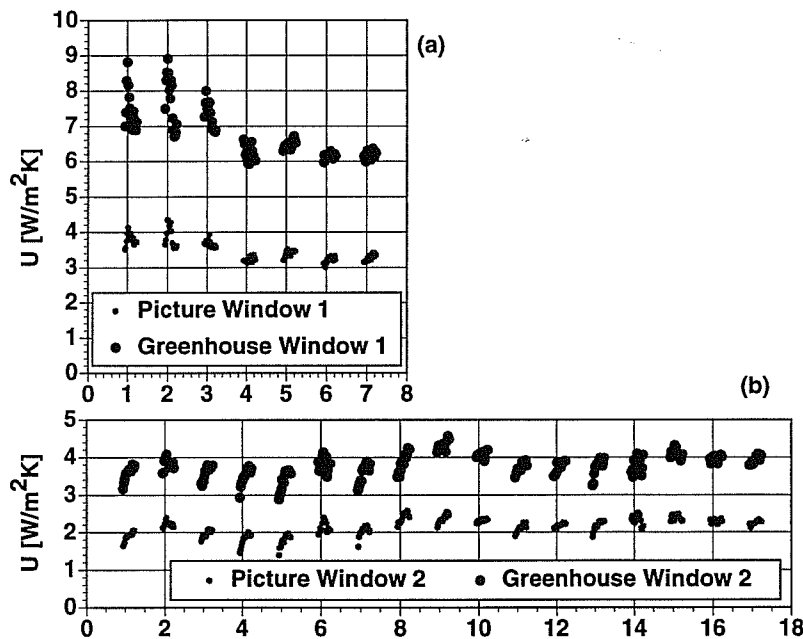


Figure 3. Measured U-Factors Verses Time. (a) First pair of test samples. (b) Second pair of test samples.

While the general variability of the U-factor appears from these plots to be on the order of 25-35%, the first three nights of Test 1 show sharply higher U-factors, particularly for the greenhouse window, and most of this increased variability also occurs within the course of each night.

The very much larger value of the greenhouse window U-factors as compared to the picture windows of similar construction is due, of course, to the use of the wall aperture (“rough opening”) rather than the surface area in defining these U-factors. Had the surface area been used, the greenhouse and picture window U-factors would have comparable magnitudes.

Time Variation of U-Factor

In Figure 4 the selected nights are displayed as a function of time, with midnight of each night taken as the zero point. These plots show that what could be taken for random fluctuation in Figure 3 resolves into definite and relatively smooth trends within each night; however, nights can be quite different from one another. For Greenhouse Window 1 one observes a large enhancement in the U-factor during the first half of the night for nights 1-3, while the remaining nights 4-7 show a relatively constant U-value. The enhancements on nights 1-3 also occur for Picture Window 1. The data for Greenhouse Window 2 show no such definite features, although different nights display quite different trends. For example, Night 5, which yields a generally low U-factor, also shows a marked variation from a low value early in the night to a higher value in the early morning. Night 9, on the other hand, always shows a higher U-factor, but the value is relatively constant throughout the night. These differences in trend are also visible in the data for Picture Window 1. Note that for nights 4 and 5, both windows show dips in their respective curves between 12:45 and 1:45 AM.

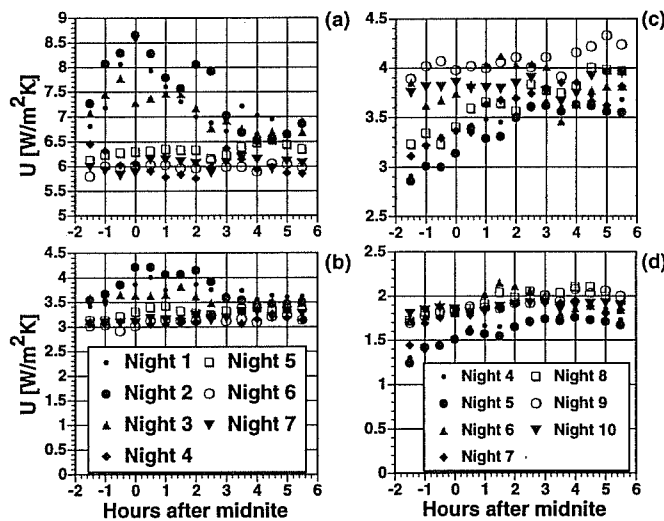


Figure 4. Measured U-Factors as a Function of Time of Night. (a) Greenhouse Window 1. (b) Picture Window 1 [simultaneous with (a)]. (c) Greenhouse Window 2. (d) Picture Window 2 [simultaneous with (c)]. Measurement uncertainties in these plots are comparable to the sizes of the large symbols.

Examination of the facility logbook for nights 1 and 2 of Test 1 indicated that those nights occurred during a snowstorm, which provides a plausible explanation of the peak in U-factor. The afternoon preceding Night 3 is listed as “sunny and windy” with no indication of snow; however, a number of similarities in the data between Night 3 and the preceding two nights lead us to suspect that there was some form of precipitation on that night as well: a high wind speed in combination with a higher than normal sky radiant temperature, which indicates that it was overcast, and sample surface temperatures that were anomalously low in relation to the exterior air temperature.

Variation of U-Factor with Exterior Conditions

The above discussion of precipitation anticipates the issue of dependence of the U-factor on exterior conditions. One can understand this effect by reference to the electrical analog models of

Figure 5. The window U-factor is normally conceptualized as shown in Figure 5(a), but the interior and exterior film resistances shown there are merely effective values representing a more complex underlying process. Part (b) of the figure shows the effect of precipitation. Droplets (or particles) of precipitation contacting the window surface result in an additional heat loss for the window surface to provide latent heat (for cold droplets), heat of fusion (for snow or ice) and heat of evaporation to the droplets. This results in a drop in the exterior surface temperature and an increase in the heat flow W through the window, which in turn results in a larger measured U-factor for the window, since

$$U_{MEAS} = \frac{W}{A_{REF} \cdot (T_i - T_o)}, \quad (1)$$

where A_{REF} is the area of the planar representation of the window, as discussed above.

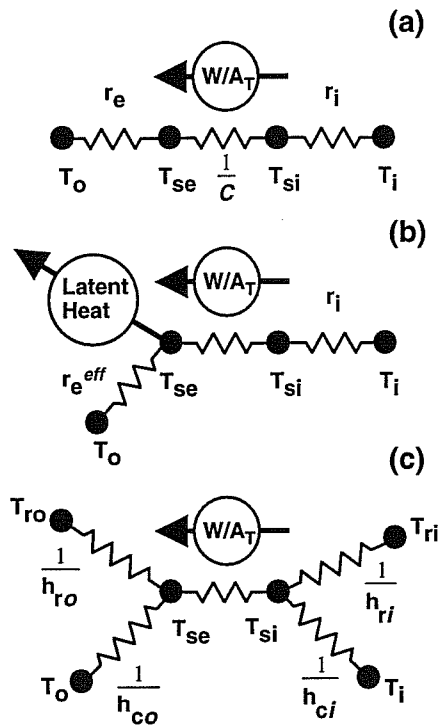


Figure 5. Electrical Analog Models of Window U-factor. (a) General Conceptual Model. T_i and T_o are the interior and exterior (effective) air temperatures, respectively; T_{se} and T_{si} are the exterior and interior surface temperatures; C is the window conductance; and r_e and r_i are the exterior and interior film resistances. W is the net heat flow through the sample, and A_T is the total surface area. (b) Effect of Precipitation. (c) Physical Model Without Precipitation. T_{ro} and T_{ri} are the exterior and interior effective radiant temperatures, h_{ro} and h_{co} are the exterior radiative and convective heat transfer coefficients, and h_{ri} and h_{ci} are the interior radiative and convective heat transfer coefficients.

When there is no precipitation, a reasonable physical model for the window is that shown in Figure 5(c), which indicates that on the exterior the glazing surface is coupled to the exterior air temperature by convection and separately by radiation to a mean radiant temperature that is in general different from the air temperature. In our measurements the mean radiant temperature is measured by a vertically mounted pyrgeometer located on the sample wall above and between the sample openings of the two calorimeters. The temperature, T_{sky} , measured by this instrument is a good approximation to the mean radiant temperature of the hemisphere (consisting approximately of half ground and half sky) viewed by a planar sample mounted in either of two calorimeters. It is not exactly equal to T_{ro} in Figure 5 for a greenhouse window, however, because the upper tilted plane views more than half the sky, while the side and bottom faces of the window view quite

different hemispheres. For the greenhouse window we use $T_{\text{sky}} - T_o$ as an indicator of the difference $T_{\text{ro}} - T_o$, rather than as a quantitative measure.

Figure 5(c) yields a qualitative understanding of the trends in our U-factor measurements. Figure 6 shows detailed information for the two most divergent nights in Figure 4(c), Nights 5 and 9. These are the two most divergent nights remaining in the data, once Nights 1-3 in Figure 4(a) (the behavior of which has been attributed to precipitation) have been excluded. In Figure 6 the data has been plotted before combining into 30-minute averages. Part (a) of the figure shows that Night 5 always measures a smaller U-factor than Night 9, with the difference between the nights smallest between 3 and 4 AM. Part (b) shows that this results from a corresponding difference in net heat flow, rather than a difference in exterior air temperature; in fact, the air temperatures on the two nights were quite similar, as can be seen from part (c). Night 9 showed a consistently somewhat lower radiant temperature (part (d)), but the major difference is the wind speed shown in part (e). The convective film coefficient for a planar sample shown in part (f) is clearly dominated by the effect of wind.

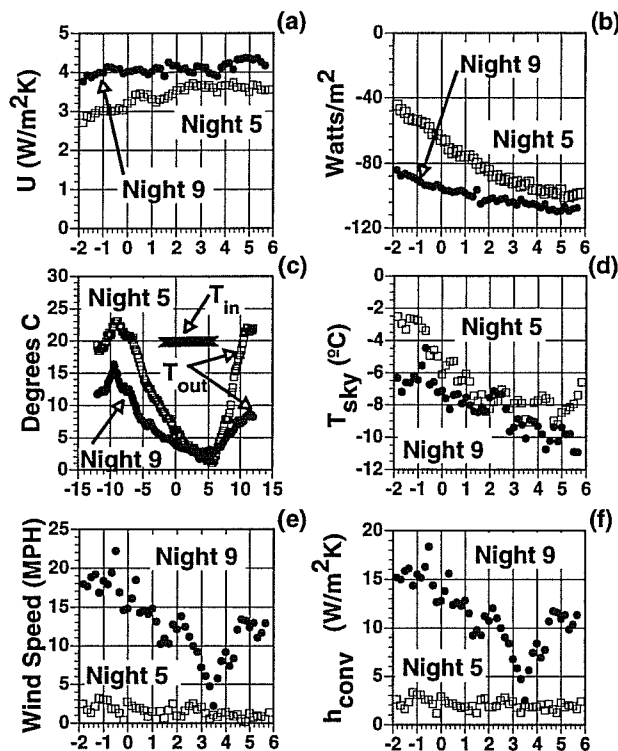


Figure 6. Greenhouse Window 2: Comparison of Nights 5 and 9. Horizontal scale is time (hrs) relative to current midnight. Data is plotted each 10 minutes. (a) Measured U-factor. (b) Net Heat Flow Through Window. (c) Interior and Exterior Air Temperatures. Note that the time scale of this plot (horizontal axis) has been expanded in order to include outdoor temperature data for the preceeding and subsequent daytimes. (d) Mean Radiant Temperature of Hemisphere Viewed by the Sample Pyrgometer. (e) On-Site Horizontal Wind Speed (10 m height). (f) Exterior Convective Film Coefficient for a Planar Window Sample. This quantity is calculated from the site horizontal wind speed, direction, and exterior air temperature, using a published formula.

One concludes, therefore, that the U-factor on Night 9 is always higher than on Night 5 because Night 9 is windy while Night 5 is relatively calm. The wind speed on Night 9 is lowest between 3 and 4 AM, and that is also when the U-factors are most nearly the same. The slope in the U-factor curve for the early part of Night 5 (see Figure 6(a)) could be due to the falling value of T_{sky} (Figure 6(d)) during the same time period; this effect could also be why the falling wind speed during that period (Figure 6(e)) on Night 9 does not cause a corresponding fall in U-factor.

Average U-Factors

Table 2 presents the average measured U-factors obtained from these tests. For Test 1 (Picture Window 1 and Greenhouse Window 1) this is an average over Nights 4-7 only, since the results for which there was precipitation have been excluded. For Test 2 the results are averaged over all 17 nights shown in Figure 1(b). These averages are, of course, dependent on the particular weather conditions encountered during the test; however, while these conditions were not extremely cold, they are probably not too dissimilar to conditions over much of the US during much of the heating season, so that they provide a useful counterpoint to hotbox test data.

The U-factor errors quoted in Table 2 are dominated by physical fluctuations in the U-factors over the course of the test period rather than by measurement error; they are essentially the standard deviations of the measured U-factors about the quoted average.

Table 2. Average Measured U-Factors

	Assumed Area (m²)	Average U-Factor (W/m² K)
Picture Window 1	1.375	3.23 ± 0.11
Greenhouse Window 1	1.520	5.57 ± 0.17
Picture Window 2	1.375	2.03 ± 0.17
Greenhouse Window 2	1.542	3.30 ± 0.22

Comparison With Hotbox Test and Simulation Results

As mentioned earlier, Greenhouse Window 1 was the subject of an ASHRAE/NFRC validation study for which test and simulation results have been published. (Carpenter and Elmahdy 1994) These results are for considerably different conditions from those encountered during this work, so some additional information will be necessary before one can make a direct comparison. The key issue is the interior and exterior film resistances defined in Figure 5.

During the outdoor test, sensors attached to the glass and framing surfaces monitored the surface temperatures. While the temperature sampling was not as complete as one might desire, it was possible to estimate the mean interior and exterior surface temperatures from the measurements. This then made possible the calculation of the effective interior and exterior film resistances, based on the measured total heat flow, the total surface area, and the air temperatures. It was found that the interior and exterior film resistances were correlated, so that the most accurate way to plot the measured data was as a function of the sum of the film resistances, as shown in Figure 7. If the surface-to-surface conductance, C , of the sample is approximately constant (as is expected theoretically), then the expected curve for this data (shown on the figure) is a straight line with slope A_{EFF} / A_T . The data is quite consistent with this. While in principle it would be possible to extrapolate this straight line to obtain $1/C$, a number of potential biases in the data make this an unreliable procedure. The plot can, however, be used to extrapolate the measurements to compare with the test and simulation data.

Table 3 lists the results of this extrapolation. The plot was used to extrapolate the measured results to the standard conditions of Carpenter and Elmahdy, and is compared with their published results

for those conditions. The error on our extrapolation is determined from the scatter of the data points about the theoretical curve in Figure 7. This error is much smaller than the corresponding one in Table 2, because it does not include the physical fluctuations in the film coefficients, except insofar as they effect the fit of the line to the data in Figure 7. Carpenter and Elmahdy's results are for a definite set of film coefficient values. The result is that the error in Table 3 ($0.02 \text{ W/m}^2\text{K}$) is essentially the statistical error of the mean value of the distribution of U-factors measured for Greenhouse Window 1, while the error value quoted in line 2 of Table 2 is the *single measurement error*. The difference between the two values is a factor of the square root of $N-1$, where N is the number of measured values. N is 56 for Table 2 and somewhat more for the data in Figure 7, which leads to Table 3.

Table 3. Greenhouse Window 1: Comparison to Published Data

	U [$\text{W/m}^2 \text{ K}$]
Test (Carpenter and Elmahdy 1994)	9.91
Simulation (Carpenter and Elmahdy 1994)	11.15
Present measurement extrapolated to standard conditions of (Carpenter and Elmahdy 1994)	8.31 ± 0.02

Our measurements are not consistent with the hotbox test results, as both are extrapolated to Carpenter and Elmahdy's standard conditions. This inconsistency is not an artifact of the extrapolation. The hotbox test results are originally formulated as a measurement of the C value, which could be used to calculate the intercept of the expected curve in Figure 7. If this were done the curve would lie above the data by much more than our experimental error, or that of the hotbox test.

As will be seen, there is good reason why the interior film coefficient should not be “adjusted” to a standard value of 8.3 for this sample. We therefore present in Figure 8 a re-plot of the data in Figure 7 as a function of the exterior film coefficient. The data points are further identified by intervals of the measured interior film coefficient. It can be seen from Figure 7 that once measured film coefficients are used the data from nights where there either was or may have been precipitation become understandable. These data points are also included in Figure 8, but are identified so that the reader may exclude them if desired. However, they provide the highest exterior film coefficient points. If we utilize the data from Nights 3-7 to estimate the U-factor for the mean observed interior film coefficient ($5.34 \pm 0.19 \text{ W/m}^2 \text{ K}$) and assume an exterior film coefficient of $29 \text{ W/m}^2 \text{ K}$, we obtain $U = 6.35 \pm 0.15 \text{ W/m}^2 \text{ K}$. In Figure 8 this point would be consistent with the nearby points in the same interior film coefficient region ($5.26 \leq h_i < 5.50 \text{ W/m}^2 \text{ K}$, inverted triangles) and below the other points with higher values of h_i , as one would expect. In another paper presented at this meeting (Arasteh, Finlayson et al. 1997) a simulation is presented that more nearly represents these conditions: $h_o=29$ and a constant interior convective coefficient are assumed, but a radiation exchange calculation over the interior surface is used to determine the mean radiant temperature. The result is closer than the previously cited simulation, but still lies above the measured value.

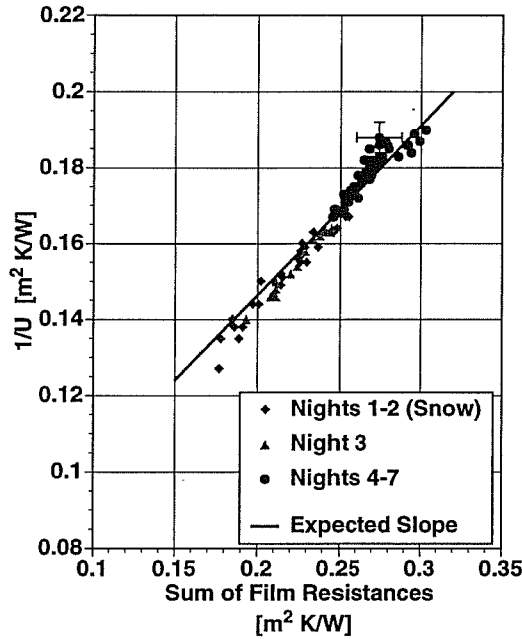


Figure 7. Greenhouse Window 1: Measured Reciprocal U-factor vs Sum of Film Resistances. The scatter of the data with respect to the line is consistent with the experimental errors, as indicated by the error bars marked on an extreme point. Data from nights with precipitation also follow the expected curve, and in fact provide all of the available data for low film resistance.

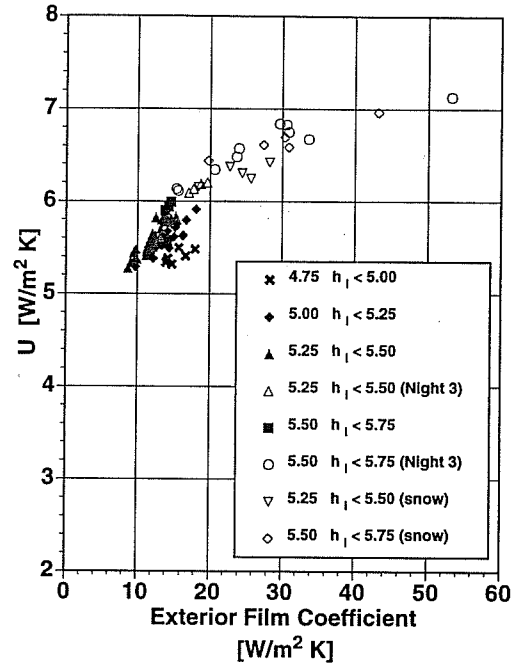


Figure 8. Greenhouse Window 1: Measured U-factor vs Exterior Film Coefficient. Data points are identified by the value of h_i , the interior film coefficient, and data from nights on which precipitation may have occurred are separately identified. The latter contribute all of the high exterior film coefficient points.

Interior and Exterior Film Coefficients

Figure 9 shows the frequency of occurrence of exterior film coefficient values over the course of Test 1. Part (a) of this figure presents the distribution for Picture Window 1 determined by two different methods. In the first method, intended to serve as a baseline and connecting link with other tests, the exterior film coefficient is derived from measurement of wind speed and exterior air temperature through a previously-determined formula (Yazdanian and Klems 1994). This method can only be used for samples that are essentially planar. In the second method, the effective exterior film coefficient for each measurement point is derived from the formula

$$h_o = \frac{W}{A_T \cdot (T_{se} - T_o)}, \quad (2)$$

where W is the measured net heat flow through the sample, A_T is the total surface area, T_{se} is the mean exterior surface temperature, and T_o is the exterior air temperature. Part (b) gives the effective film coefficient for Greenhouse Window 1, derived by the second method. Both plots in Figure 9 include data from Nights 3-7. The inset in Figure 9b shows the effect on that plot of displaying higher resolution and excluding Night 3; the chief effect is to remove the high-film-coefficient “tail” on the distribution.

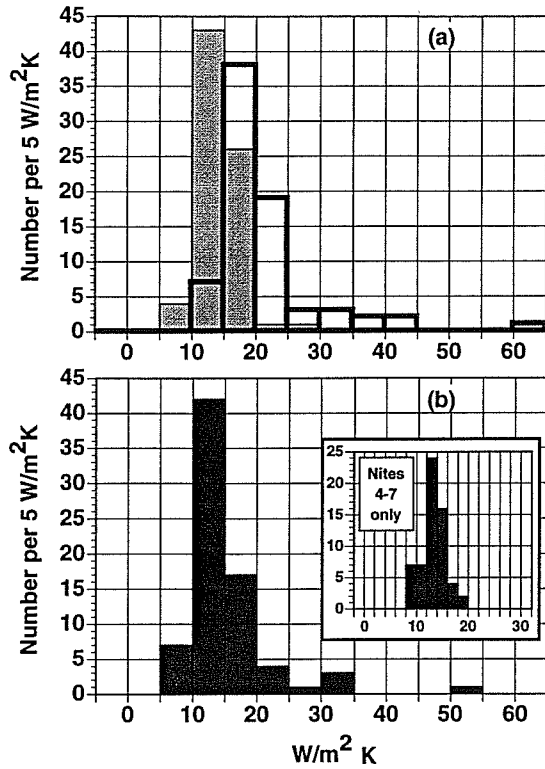


Figure 9. Frequency Distribution of Exterior Film Coefficient. (a) Picture Window 1. The exterior film coefficient is derived by two alternative methods. Shaded histogram: Values derived from measured wind speed, exterior air temperature, and glazing surface temperature using a published formula. Open histogram: Values derived by same method as for Greenhouse Window 1. (b) Greenhouse Window 1. Exterior film coefficient is derived from the measured mean exterior surface temperature, the exterior air temperature, the heat flow through the sample, and the total exterior surface area. Data from nights 3-7 are included in the plots. The inset shows the distribution when night 3 is excluded.

The difference between the two distributions in Part (a) gives a check on the uncertainty in determining the absolute value of the exterior film coefficient: There is an uncertainty on the order of $5 \text{ W/m}^2 \text{ K}$. (The tail on the distribution of the open histogram due to precipitation of course cannot be obtained using the method of the shaded histogram.) This uncertainty does not affect a comparison between the open histogram in Part (a) and the histogram in Part (b); both of these distributions were obtained by the same method. One can conclude that the mean exterior film coefficient experienced by the greenhouse window is somewhat lower than that experienced by the picture window. This is a result somewhat counter to expectations. It may be due to the geometry of the greenhouse window, or it may simply be an artifact of the window's having a significant area (the lower "shelf") that is wood, not glazed, and which faces the ground. To resolve this question would require detailed simulation of the measurement conditions, and also a greater amount of detail in the measurements.

Figure 10 presents a similar comparison of interior film coefficients derived for Picture Window 1 and Greenhouse Window 1 using

$$h_i = \frac{W}{A_T \cdot (T_i - T_{si})}, \quad (3)$$

where T_i is the interior air temperature and T_{si} is the mean interior surface temperature of the sample. While the planar picture window shows the expected interior film coefficient of approximately $8 \text{ W/m}^2 \text{ K}$, the greenhouse window exposed to the same calorimeter room interior conditions experiences a significantly lower interior film coefficient. This must, at least in part, be due to the radiative effect mentioned earlier: because individual panels of the greenhouse window view other window panels as well as the (warmer) calorimeter interior, the effective radiant

temperature, T_{ri} , of Figure 5(c) should be lower, resulting in a lower interior film coefficient. Because of the difference in geometry between the greenhouse window and an essentially planar window, one would expect that the convective coefficient, h_c , would also be different, but the sign of the difference is not so apparent. In any case, it is clear that the assumption of a “standard” interior film coefficient in the neighborhood of $8 \text{ W/m}^2 \text{ K}$ is unwarranted for this type of window.

Conclusions

There is not yet a satisfactory convergence between hotbox measurement, field measurement, and simulation on a method of determining the U-factor for a projecting product such as a greenhouse window.

It is not uncommon for field measurements to yield significantly lower U-factors than hotbox tests on the same conventional window. This is an expectable result of the conditions imposed in the hotbox test, and when detailed account is taken of the differences in imposed conditions, it is normal to find that the two sets of tests agree to relatively high accuracy. Based on published data and the hotbox test report (Carpenter and Elmahdy 1997) for Greenhouse Window 1, no such agreement is possible.

The interior heat transfer coefficient that occurs in a greenhouse window has been shown to be significantly lower than that of a substantially planar window subjected to the same “still air” conditions. This circumstance may complicate the interpretation of hotbox tests, and means that simulations assuming “standard” interior conditions produce U-factors that are too high.

Acknowledgments

This work was supported by the Assistant Secretary for Energy Efficiency and Renewable Energy, Office of Building Technology, State and Community Programs, Office of Building Systems of the U.S. Department of Energy under Contract No. DE-AC03-76SF00098.

The efforts of Dennis DiBartolomeo, Guy Kelley, Michael Streczyn, and Mehrangiz Yazdanian were vital to support of the test facility and to carrying out these tests. We are indebted to the Experimental Farm, University of Nevada at Reno, for their hospitality in providing a field site and for their cooperation in our activities.

References

- Arasteh, D., M. S. Reilly, et al. (1989). “A Versatile Procedure for Calculating Heat Transfer Through Windows.” ASHRAE Trans. **95**(2).
- Arasteh, D. K., E. U. Finlayson, et al. (1997). “Guidelines for modeling projecting fenestration products.” ASHRAE Trans. **104**(1): to be published.
- Bowen, R. P. (1985). DBR's approach for determining the heat transmission characteristics of windows, Institute for Research in Construction, National Research Council Canada.
- Bowen, R. P. and K. R. Solvason (1984). A calorimeter for determining heat transmission characteristics of windows. ASTM Conference on Thermal Insulation, Materials and Systems, Dallas.
- Carpenter, S. C. and A. H. Elmahdy (1994). “Thermal Performance of Complex Fenestration Systems.” ASHRAE Trans. **100**(Pt. 2): 1179-86.

- Carpenter, S. C. and A. H. Elmahdy (1997). personal communication.
- Childs, K. W. (1991). HEATING 7.1 User's Manual. Oak Ridge, TN, Oak Ridge National Laboratory.
- Elmahdy, A. H. (1992). "Heat Transmission and R-value of Fenestration Systems Using IRC Hot Box: Procedure and Uncertainty Analysis." ASHRAE Trans. **98**(Pt. 2): 630-37.
- Elmahdy, A. H. and R. P. Bowen (1988). "Laboratory Determination of the Thermal Resistance of Glazing Units." ASHRAE Trans. **94**(pt. 2): 1301-16.
- EE. 1989. FRAME, A finite-difference computer program to evaluate thermal performance of window systems. Waterloo, Ontario, Canada, Enermodal Engineering, Ltd.
- Finlayson, E., D. Arasteh, et al. (1996). Therm 1.0: Program Description: A PC Program for Analyzing the Two Dimensional Heat Transfer Through Building Products, E. O. Lawrence Berkeley National Laboratory, Report LBL-37371 Rev., Berkeley, CA 94720.
- Finlayson, E. U., D. K. Arasteh, et al. (1993). WINDOW 4.0: Documentation of Calculation Procedures, Lawrence Berkeley Laboratory, Report LBL-33943, Berkeley, CA 94720.
- Klems, J. H. (1992). "Method of Measuring Nighttime U-Values Using the Mobile Window Thermal Test (MoWiTT) Facility." ASHRAE Trans. **98**(Pt. II): 619-29.
- Klems, J. H., S. Selkowitz, et al. (1982). A Mobile Facility for Measuring Net Energy Performance of Windows and Skylights. Proceedings of the CIB W67 Third International Symposium on Energy Conservation in the Built Environment. Dublin, Ireland, An Foras Forbartha. **III**: 3.1.
- Mitalas, G. P. (1968). "Calculation of Transient Heat Flow Through Walls and Roofs." ASHRAE Trans. **74**(Pt. 2): 181.
- NFRC (1991). NFRC 100-91: Procedure for Determining Fenestration Product Thermal Properties (Currently Limited to U-Value). National Fenestration Rating Council, Silver Spring, MD.
- Yazdanian, M. and J. H. Klems (1994). "Measurement of the Exterior Convective Film Coefficient for Windows in Low-Rise Buildings." ASHRAE Trans. **100**(pt. 1): 1087-1096.